Arch. Pharm. Chem. Life Sci. 2017, *350*, e1600304

ARCH PHARM
Archiv der Pharmazie

Full Paper

An Efficient Synthesis of *bi*-Aryl Pyrimidine Heterocycles: Potential New Drug Candidates to Treat Alzheimer's Disease

Tanzeel Ur Rehman[1], Islam Ullah Khan[1], Muhammad Ashraf[2], Hamadeh Tarazi[3], Sadaf Riaz[1], and Muhammad Yar[4]*

[1] Department of Chemistry, GC University, Lahore, Pakistan
[2] Department of Chemistry, The Islamia University of Bahawalpur, Bahawalpur, Pakistan
[3] Department of Medicinal Chemistry, College of Pharmacy, University of Sharjah, Sharjah, UAE
[4] Interdisciplinary Research Center in Biomedical Materials, COMSATS Institute of Information Technology, Lahore, Pakistan

A series of 13 novel pyrimidine-based sulfonamides **6a–m** were synthesized in short periods of time under microwave conditions in good to excellent yield (54–86%). The chemical structures of these heterocycles consist of a central pyrimidine ring having a phenyl group and pyrimidine groups with sulfonamide motifs. The enzyme inhibitory potential of these compounds was investigated against acetylcholinesterase (AChE) and butyrylcholinesterase (BChE) because these enzymes play a crucial role in the treatment of Alzheimer's disease. As compared to the reference compound eserine ($IC_{50} = 0.04 \pm 0.0001\ \mu M$ for AChE and $IC_{50} = 0.85 \pm 0.0001\ \mu M$ for BChE), the IC_{50} values of the synthesized compounds ranged from $3.73 \pm 0.61\ \mu M$ to $57.36 \pm 0.22\ \mu M$ for AChE and $4.81 \pm 0.16\ \mu M$ to $111.61 \pm 0.53\ \mu M$ for BChE. Among these tested compounds, **6j** having a $-CH_3$ group was found to be the most potent one against both enzymes (AChE, $IC_{50} = 3.73 \pm 0.61\ \mu M$; BChE, $IC_{50} = 4.81 \pm 0.16\ \mu M$). Quantitative structure–activity relationship (QSAR) and molecular docking studies of the synthesized compounds were also performed.

Keywords: AChE / Alzheimer's disease / BChE / Pyridine / Pyrimidines / Sulfonamides

Received: October 20, 2016; Revised: January 15, 2017; Accepted: January 16, 2017

DOI 10.1002/ardp.201600304

Additional supporting information may be found in the online version of this article at the publisher's web-site.

Introduction

Alzheimer's disease (AD) is a widely spreading neurodegenerative disease. About 35.6 million people world-wide have been affected from this disease [1–3] which is caused due to the death of brain cells. The most common symptoms of AD are gradual loss of memory, judgment, and learning potential [4, 5]. It is believed that the acetylcholinesterase (AChE) has important contribution in the normal function of cholinergic system and is associated with AD through its contribution in the acetylcholine metabolism [6]. In addition, cholinergic neurotransmission is also co-regulated by butyrylcholinesterase (BChE), which becomes more active during AD.

Recent therapeutical agents to inhibit AChE and BChE [7–9] are donepezil [10], rivastigmine [11], and galantamine [12] belonging to the class of cholinesterase inhibitors [13]. These cholinesterase inhibitors have various issues including central and peripheral side effects. Clinical studies have indicated that tacrine has hepatotoxic liability [14] and due to inauspicious events, it was ceased [15]. Studies have revealed that inhibition of AChE-induced Aβ aggregation [16] by cholinesterase inhibitors employ additional benefits for AD treatment

Correspondence: Dr. Muhammad Yar, Interdisciplinary Research Center in Biomedical Materials, COMSATS Institute of Information Technology, Lahore 54000, Pakistan.
E-mail: drmyar@ciitlahore.edu.pk

*Additional correspondence: Prof. Islam Ullah Khan,
E-mail: iuklodhi@yahoo.com

[17, 18]. In recent years, a significant number of studies have shown the positive role of dual cholinesterase inhibitors (AChE and BChE) to treat AD [19, 20]. Common AChE and BChE inhibitors like isosorbide, thienthiazine, and diarylimidazoles are responsible for the declines in cognitive, behavioral, and global functioning characteristics of AD [21–27].

Pyrimidines are the most significant class of the heterocycles in medicinal chemistry. Recently, these compounds have attracted much attention and especially amino substituted pyrimidine derivatives delivered a wide range of pharmacological effects like antibacterial [28], antifungal [29], antidepressant [30], antitumor [31, 32], and antiviral [33, 34]. Sulfonamides constitute nearly 300 drugs currently in the market. Numerous sulfonamide-based medicines have been developed as diuretics, anti-migraine agents, cyclooxygenase-II (COX-2)-specific anti-inflammatory activities [35, 36]. In addition, aromatic heterocyclic sulfonamides possessing free amino function have shown effective inhibition of three carbonic anhydrase isozymes [37].

Promising biological activities of pyrimidines, sulfonamides, and our recent contribution in this field [38, 39] have prompted us to synthesize and investigate the cholinesterase inhibition potential of a range of novel pyrimidine-based sulfonamides. Although, putting bi-aryl groups in the pyrimidine ring is quite challenging, so we have adopted a simple and straight forward strategy which has delivered good yields and unique inhibition activities.

Results and discussion

Chemistry

As a result of extensive literature search, we could not find any pyridine substituted pyrimidines. In this study, a series of structurally related pyridine pyrimidine sulfonamides (**6a–m**) were synthesized by conventional and microwave assisted synthetic strategy as outlined in Table 1. Microwave activation as a non-conventional energy source has been adapted to the assembly of a library of compounds. This protocol has the advantage of better yields, significant purity, less time span, and environmental friendly process than conventional heating method where delayed reaction time causes the decomposition most of the reactions. These results confirm the applicability of microwave heating to the improvement of classic reactions. Condensation of 4-phenyl-6-(pyridin-3-yl pyrimidin-2-amine (**5**) with substituted sulfonyl chlorides in DMF at room temperature, using pyridine as a base. The products were recrystallized from methanol to get essentially pure products (**6a–m**) in good to excellent yields by microwave (54–86%) and conventional (52–83%) strategy.

Biological evaluations

AChE and BChE inhibition

Primarily electronic and steric effects were found to be responsible for varying the activity against the enzymes. To study the structure–activity relationship of this class, we compared the activities of 13 analogs (**6a–m**) with different electron donating and withdrawing groups. All synthesized compounds (**6a–m**) were screened for their *in vitro* inhibition against AChE and BChE using commercially available eserine as control. The results summarized in Table 2 indicate that parent compound **5** was completely inactive while compounds **6j**, **6k**, **6i**, and **6g** were found to be potent against AChE and compounds **6j**, **6i**, and **6m** showed average inhibition against BChE as compared to others with minimum affinity. Compounds **6i** and **6j** exhibited the most desired results against both enzymes.

In case of AChE activity, compound **6a** possessing bromo at C-2′ of the phenyl ring exhibits weak inhibition with IC_{50} value ($57.36 \pm 0.22\,\mu M$). This inhibition activity further enhanced as in compound **6c** (IC_{50} $38.36 \pm 0.29\,\mu M$) where phenyl ring possesses bromo at C-4′, while bromo at C-3′ makes the compound **6b** inactive. This indicated that *ortho* and *para* positions played significant role for the higher activity in **6a** and **6c** compounds. Removal of bromo group from phenyl ring yielding **6m**, moderately improved the activity (IC_{50} $34.21 \pm 0.78\,\mu M$) as compared to **6a** and **6c.** This hypothesis was further supported by the observation of increased activity in the case of compound **6i.** Replacement of bromo moiety with CH_3 at C-4′ of phenyl ring yielding **6i**, actively improved the activity (IC_{50} $9.21 \pm 0.31\,\mu M$) and make it third most active among synthesized compounds against AChE. CH_3 group at C-2′, as in compound **6g** (IC_{50} $21.42 \pm 0.11\,\mu M$), again decreased the inhibition. While same group at C-3′ made compound **6h** inactive. Surprisingly, the activity of compound **6k** (IC_{50} $6.11 \pm 0.65\,\mu M$) increased enormously when substituted phenyl ring of sulfonyl group was replaced by ethyl group. Whereas, compound **6j** (IC_{50} $3.73 \pm 0.61\,\mu M$), possessing CH_3 moiety attached with sulfonyl group turned out to be the most potent among the compounds screened for AChE inhibition. This revealed that electron releasing moiety is crucial for the higher activity of **6j**. Rest of the compounds with chloro, bromo, and nitro moieties over phenyl ring were less active or inactive, due to electron withdrawing effect of substituents.

In case of BChE inhibition studies, compound **6j** (IC_{50} $04.81 \pm 0.16\,\mu M$) was turned out to be the most active. The higher activity of **6j**, bearing methyl moiety bonded to sulfonyl group, showed a similar trend against AChE inhibition. Compounds **6i** (IC_{50} $20.11 \pm 0.41\,\mu M$), **6m** (IC_{50} $36.83 \pm 0.84\,\mu M$), and **6c** (IC_{50} $40.19 \pm 0.11\,\mu M$) have shown moderate activities whereas the rest of the compounds showed either low activity or were inactive against BChE. Generally, it was noticed that pyrimidines containing small alkyl groups exhibited higher activities than aryl and higher alkyl gorups.

Molecular modeling

QSAR analysis

To further explore the contribution of different structural features exhibited by the compounds in relation to AChE and

Table 1. Synthetic conditions for pyridine pyrimidine sulfonamides (6a–m) and yields.

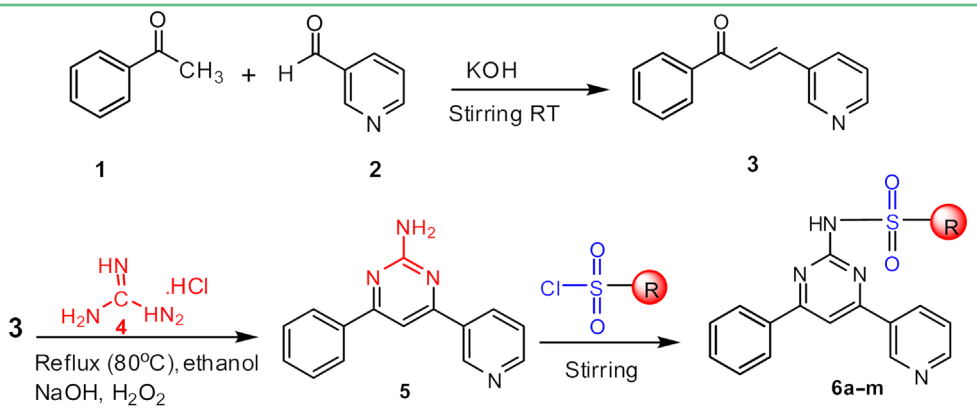

Compound	R	Yield %	Compound	R	Yield %
6a		69[a] (68)[b]	6h	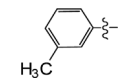	78[a] (76)[b]
6b		71[a] (69)[b]	6i	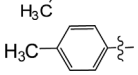	86[a] (83)[b]
6c	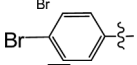	82[a] (81)[b]	6j		79[a] (77)[b]
6d		73[a] (71)[b]	6k		80[a] (79)[b]
6e	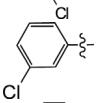	69[a] (64)[b]	6l	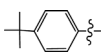	54[a] (52)[b]
6f	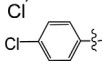	77[a] (77)[b]	6m		59[a] (55)[b]
6g		61[a] (60)[b]			

[a] Microwave yield.
[b] Conventional yield.

BChE bioactivities (% inhibition), we developed two quantitative structure–activity relationship (QSAR) models. QSAR is a technique commonly used in medicinal chemistry for constructing statistically valid equations in an attempt to quantitatively link variables derived from chemical structures with any desired endpoint (i.e., biological activity). The knowledge furnished by such models unveils the structural trends present within set of compounds, and enables more rational future development.

The best developed model capable of describing the inhibitory pattern exerted by our compounds against the AChE is illustrated by Eq. (1).

$$Log(\%\text{Inhibition}) = 4.425 + 0.271 \times SM1_{Dzp} - 2.998 \times GGI8 - 0.971 \times MOMI_{YZ} + 1.197 \times L3m \quad (1)$$

$n = 20$, F-Statistic $= 49.93$, $R^2 = 0.930$, $Q^2_{LOO} = 0.876$, $Q^2_{LMO} = 0.846$, $R^2_{Y\text{-scr}} = 0.209$, $s = 0.149$

where $SM1_{Dzp}$ is first order spectral moment from Barysz matrix weighted by polarizabilities; $GGI8$ is the topological charge index of order 8; $MOMI_{YZ}$ is the moment of inertia along the Y,Z axis and $L3m$ is the third component size directional WHIM index weighted by relative mass.

On the other hand, the best performing model against BChE is illustrated by Eq. (2).

$$Log(\%\text{Inhibition}) = 5.739 + 445.612 \times ATTSC_{1c} + 3.823 \times MATS_{5p} - 3.025 \times GGI10 - 0.055 \times RDF_{45s} \quad (2)$$

$n = 20$, F-Statistic $= 64.46$, $R^2 = 0.945$, $Q^2_{LOO} = 0.91$, $Q^2_{LMO} = 0.893$, $R^2_{Y\text{-scr}} = 0.205$, $s = 0.121$

where $AATSC_{1c}$ is the average centered Broto–Moreau autocorrelation of lag 1 weighted by charges; $MATS_{5p}$ is the Moran autocorrelation of lag 5 weighted by polarizabilities; $GGI10$ is the topological charge index of order 10

Table 2. AChE and BChE inhibitions and IC_{50} values (mean ± SEM) of pyridine pyrimidine sulphonamides (6a–m).

Compd.	AChE inhibition		BChE inhibition	
	Inhibition (% ± SEM[a]) at 0.5 mM	IC_{50} (μM ± SEM[a])	Inhibition (% ± SEM[a]) at 0.5 mM	IC_{50} (μM ± SEM[a])
5	12.68 ± 0.14	ND	25.26 ± 0.23	ND
6a	74.66 ± 0.27	57.36 ± 0.22	9.81 ± 0.28	ND
6b	4.36 ± 0.27	ND	11.31 ± 0.28	ND
6c	79.36 ± 0.27	38.36 ± 0.29	79.51 ± 0.28	40.19 ± 0.11
6d	43.32 ± 0.41	<400	31.10 ± 0.29	<400
6e	32.32 ± 0.41	<400	4.29 ± 0.17	<400
6f	50.32 ± 0.41	<400	55.11 ± 0.36	<400
6g	86.87 ± 0.67	21.42 ± 0.11	73.37 ± 0.26	43.61 ± 0.11
6h	47.12 ± 0.62	<400	33.23 ± 0.92	ND
6i	89.33 ± 0.94	9.21 ± 0.31	86.37 ± 0.26	20.11 ± 0.41
6j	93.89 ± 1.19	3.73 ± 0.61	92.38 ± 1.13	4.81 ± 0.16
6k	91.06 ± 0.13	6.11 ± 0.65	68.94 ± 0.99	111.61 ± 0.53
6l	52.04 ± 0.23	<500	53.66 ± 0.39	<500
6m	79.35 ± 0.14	34.21 ± 0.78	83.76 ± 0.99	36.83 ± 0.84
Eserine[b]	**91.27 ± 1.17**	**0.04 ± 0.0001**	**82.82 ± 1.09**	**0.85 ± 0.0001**

ND, not determined.
[a]All readings were performed in triplicates and averaged, and SEM is standard mean error of the experiments.
[b]Standards used.

and RDF_{45s} is the radial distribution function-045 weighted by relative I-state.

Both models were found to fit the experimental observations (% inhibition) of AChE (Eq. 1, Fig. 1a) and BChE (Eq. 2, Fig. 1b) with considerable level of significance as indicated by their high Fischer's value (*F*), squared correlation coefficients (R^2) and the standard errors of estimate. The models presented by Equations (1) and (2) are specific to our compound's chemotype, thus their internal predictive power is judged based on leave-one-out (LOO) and leave-many-out (LMO) procedures. The probability of chance correlation is examined by the *Y*-scrambling procedure, where lower

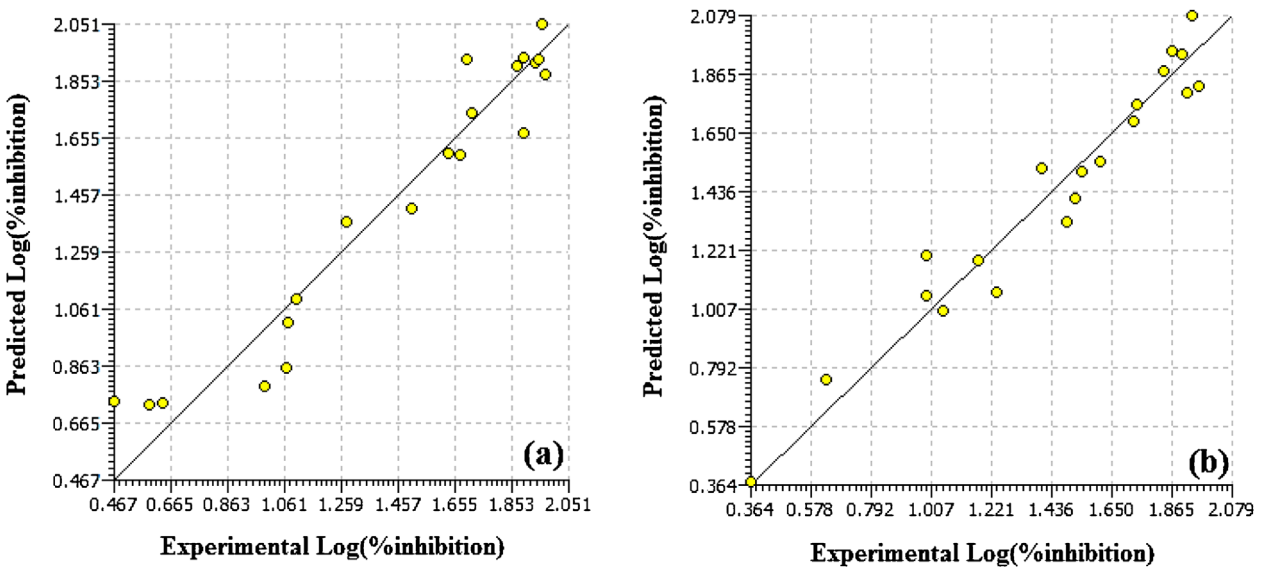

Figure 1. Scatter plot of (a) experimental versus predicted bioactivities derived from AChE QSAR equation, (b) experimental versus predicted bioactivities derived from BChE QSAR equation.

($R^2_{Y\text{-}Scr}$) value indicates lesser probability of chance correlation. The internal validation parameters achieved by both models demonstrated their reliability and robustness in predicting new derivatives within our series and could be utilized for future development.

Docking and molecular dynamics

At the next level of our investigation, we turned our focus toward the most potent compound (**6j**) in our series for detailed exploration of its binding pattern within the active sites of AChE and BChE. We commenced our study by performing rigid-body docking of **6j** against both enzymes. The docking results showed that **6j** was capable of establishing two hydrogen-bond interactions with the peripheral anionic site (PAS) residue Tyr121 upon binding to AChE (Fig. 2a). Additionally, the docked complex of BChE with **6j** (BChE-**6j**) showed that the hydrophobic patch residue Tyr128 and the catalytic triad residue Ser198 were involved in intramolecular hydrogen bonding (Fig. 2b). While docking technique is considered efficient in accurately predicting binding mode of small molecules; however, it suffers from a number of drawbacks summarized by its limited description of protein motion; effect of biological conditions. Docking procedure describes one snapshot during the protein–ligand interaction time course (frame 0), assuming that such complex resembles the most energetically favorable one. Such drawbacks could be overcome by employing molecular dynamic simulation. Accordingly, we decided to carry out 20 ns MD run to resemble the physiological conditions that would encounter the previously docked complexes in an attempt to disclose further vital binding information of our compound.

The RMSD values given in Fig. 3a and 3b showed that both systems (AChE-**6j** and BChE-**4p**) were relatively stable during the MD experiment, and they had reached equilibration by the end of the simulation period as indicated by their minor fluctuations (i.e., less than 3 Å) in the protein Cα-atoms. Based on that, the results emerged could be reliably used for binding mode analysis.

An analysis of **6j** interaction with respect to AChE amino acid residues (Fig 4a) disclosed a number of important interactions. The compound **6j** showed ability to form direct and indirect (water bridge) hydrogen bonding with the residues Asn85, Ser122 as well as with the peripheral anionic site residues Tyr121 and Tyr334 for considerable fraction of time during the simulation period. On the other hand, **6j** showed significant hydrophobic interactions with Trp84, Phe330, Phe331, and Tyr334 residues within the hydrophobic patch region (Fig 4a).

The binding pattern of **6j** with the BChE active site turned out to be more interesting, where **6j** was able to form direct hydrogen bonding with the residues Gly115, Gly116, Gly117, and Glu197 of the oxyanion hole for about 86%, 45%, 20%, 39% of the simulation time, respectively. **6j** showed significant (100%) hydrogen bond interaction with the catalytic triad residue Ser198. Additionally, it interacts with Glu197 via ionic interaction for about 12% of the simulation time, which suggest its role in ligand selectivity. The rest of the interactions are hydrophobic with Trp82, Ala199, Trp231, Phe329m and Ile442 residues established for about 59%, 13%, 33%, 17%, and 25% of the simulation time, respectively.

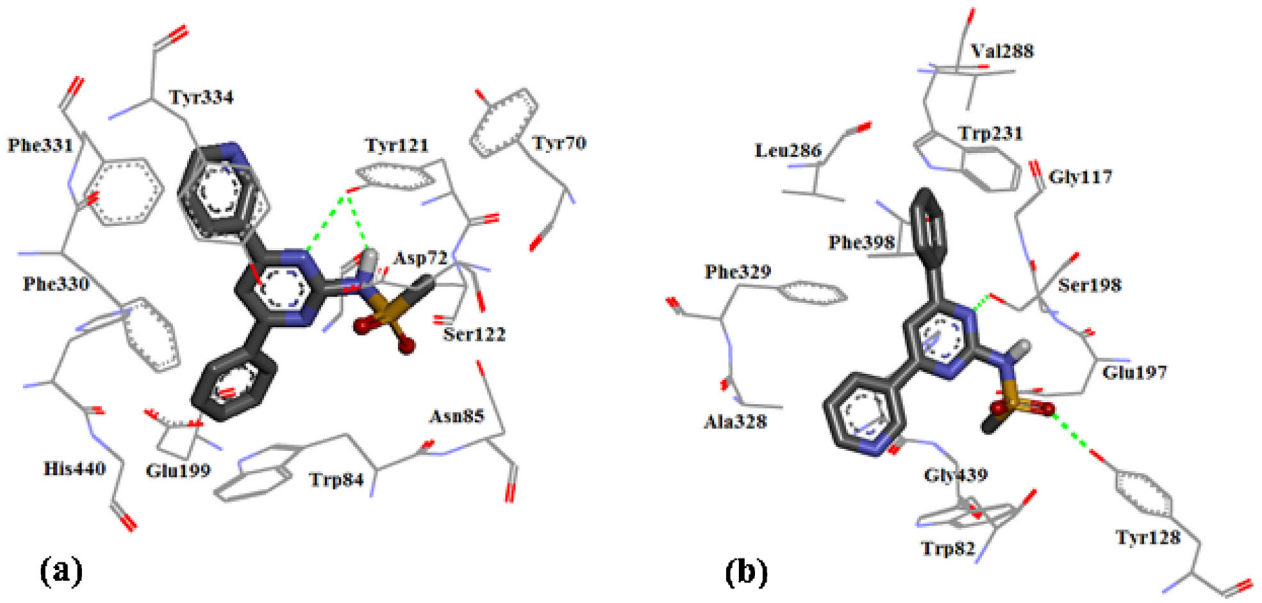

Figure 2. Best docked pose of compound **6j** within (a) the AChE active site, and (b) the BChE active site. Green dashed lines represent hydrogen bond interactions.

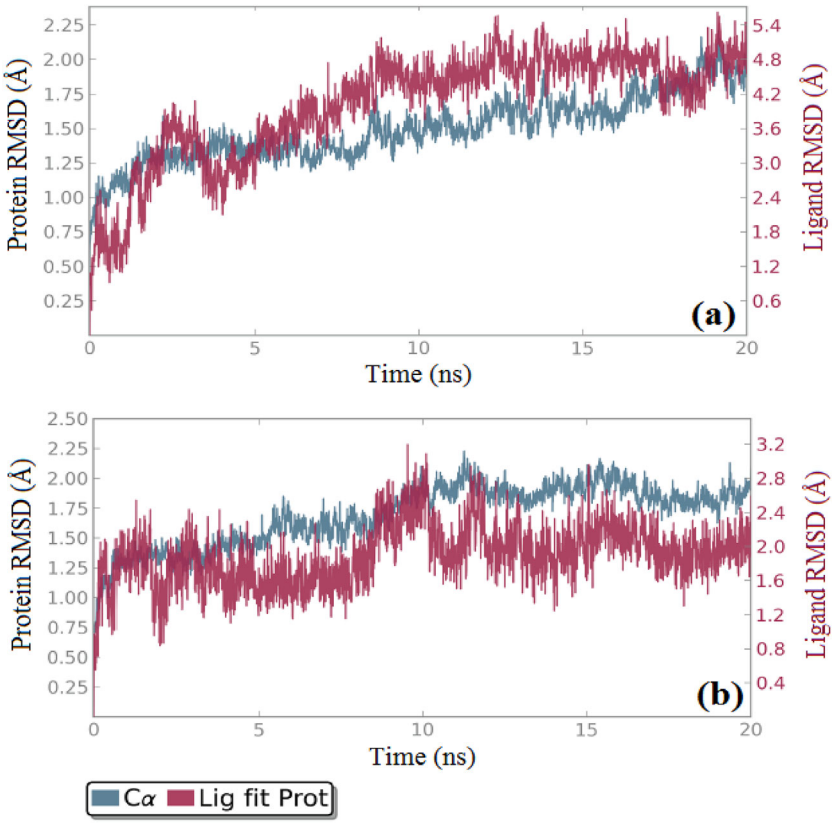

Figure 3. Protein–ligand RMSD values over the 20 ns simulation time. (a) RMSD plot for AChE Cα-atoms (blue) and compound **6j** heavy atoms (red). (b) RMSD plot for the BChE Cα-atoms (blue) and compound **6j** heavy atoms (red).

Conclusion

In this research, we have successfully prepared pyridine ring bearing sulfonamides by applying microwave assisted strategy for generating chemical diversity in the structures of pyrimidines family. The major impact of this research has been shown by synthesizing a number of novel molecules and analyzing their inhibition potential against two leading enzymes responsible for AD. Detailed *in vitro* studies showed that compound **6j** with IC_{50} value 3.73 ± 0.61 for AChE and 4.81 ± 0.16 for BChE was the most active among this series. The molecular modeling studies were focused for this compound **6j** to predict its binding modes with the respective enzyme's active sites. This paper contains a facile methodology to prepare compounds against Alzheimer's disease in good yields and short reaction time.

Experimental

Chemistry

General

All chemicals and solvents used were of analytical grade and were purchased from Sigma–Aldrich and Merck Chemical Company and were used without further purification. TLC was run on the silica-coated aluminum sheets (silica gel 60 F254, E. Merck, Germany). Microwave irradiation was carried out in a modified commercial microwave oven under atmospheric pressure. IR spectra in KBr pellets were recorded on the FT-IR Perkin Elmer spectrum BX spectrophotometer. ^{1}H NMR and ^{13}C NMR spectra were recorded at 400 and 100 MHz, respectively, on a JEOL-Lambda NMR instrument. Chemical shifts are quoted as ppm and the coupling constants *J* in Hz. Signals are described as s (singlet), d (doublet), m (multiplet), and br (broad). Melting points were measured on a Buchi 434 melting point apparatus and are uncorrected. Combustion analysis was performed on a Elementar, variomicrocube, Germany.

The InChI codes and some biological activity data of the investigated compounds are provided as Supporting Information.

*Synthesis of (E)-1-phenyl-3-(pyridin-3-yl)prop-2-en-1-one (**3**)*

(*E*)-1-Phenyl-3-(pyridin-3-yl)prop-2-en-1-one **3** was prepared using a reported method [40]. To a solution of acetophenone (1.0 equiv) and aldehyde (1.0 equiv) in ethanol was added 50% KOH (2.5 equiv) at 0°C. The mixture was stirred for 4 h at room temperature and then poured into ice water. The pH of this mixture was adjusted to 7 by using 2 M HCl aqueous

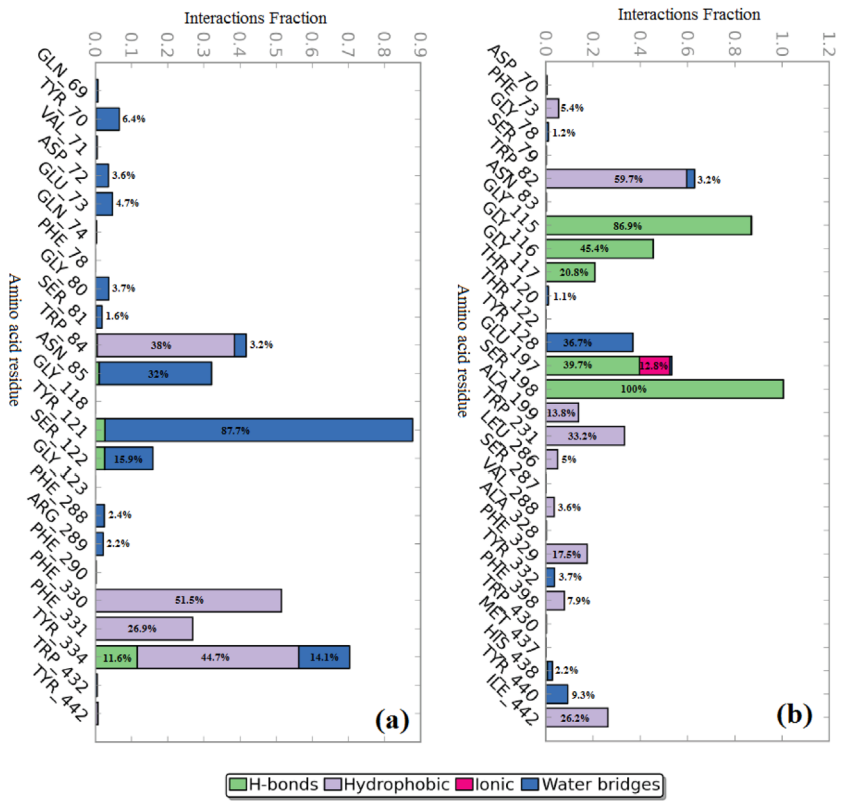

Figure 4. The fraction of interactions occurred over the simulation period between (a) compound **6j** and AChE active site. (b) Compound **6j** and the active site of BChE.

solution. Yellow precipitates of desired compound **3** were collected by filtration and purified by recrystallization in absolute ethyl alcohol. Yellow solid; yield: 79%; m.p. 123–125°C; IR (ν_{max}, KBr pellets, cm^{-1}): 3018 (C-H), 1710 (C=O), 1660 (C=C): ^{1}H NMR (DMSO-d_6) δ_H: 9.21 (1H, s, ArH), 8.27 (1H, d, $J = 9.6$ Hz, ArH), 8.22 (1H, d, CH), 7.78 (1H, d, $J = 8.0$ Hz, ArH), 7.69 (2H, d, $J = 10.8$ Hz, ArH), 7.59 (1H, t, $J = 8.0$ Hz, ArH), 7.21–7.30 (3H, m, ArH), 6.98 (1H, d, $J = 8.0$, –CH), ^{13}C NMR (DMSO-d_6) δ_H: 189.6 (1 × C), 149.3 (1 × C), 148.1 (1 × C), 142.2 (1 × C), 137.4 (1 × C), 134.7 (1 × C), 132.7 (1 × C), 129.4 (3 × C), 128.7 (2 × C), 124.1 (2 × C); Anal. calcd. for $C_{14}H_{11}NO$: C, 80.36; H, 5.30; N, 6.69; O, 7.65. Found: C, 80.50; H, 5.46; N, 6.59.

*Synthesis of 4-phenyl-6-(pyridin-3-yl)pyrimidin-2-amine (**5**)*

(*E*)-1-Phenyl-3-(pyridin-3-yl)prop-2-en-1-one **3** (45.4 mmol), guanidine hydrochloride (68.05 mmol), ethanol (100 mL), and 50% aqueous KOH solution (20 mL) were mixed together then heated up and stirred at reflux temperature for 1.5 h. Under the same conditions, 30% aqueous H_2O_2 (15.5 mL, ca. 151.5 mmol) was added to the above mixture in small portions over a period of 1.5 h. The ethanol was removed under reduced pressure in a rotary evaporator and water (100 mL) was added to the residue. The precipitated title compound was filtered off, washed thoroughly on the funnel with pure water in more cycles, and carefully drawn off. The slightly still wet crude solid was re-crystallized from ethanol and the so-obtained pure, crystalline product was dried finally in a vacuum desiccator over P_2O_5/KOH. Light yellow solid; yield: 73%; m.p. 180–182°C; IR (ν_{max}, KBr pellets, cm^{-1}): 3190 (N–H), 1194 (C–N); ^{1}H NMR (DMSO-d_6) δ_H: 9.23 (1H, s, ArH), 9.01 (1H, d, $J = 7.6$ Hz, ArH), 8.97 (1H, s, ArH), 8.81 (1H, d, $J = 8.4$ Hz, ArH), 8.70 (2H, d, $J = 9.2$ Hz, ArH), 8.61 (1H, t, $J = 7.6$ Hz, ArH), 8.26 (2H, t, $J = 8.8$ Hz, ArH), 8.01 (1H, t, $J = 11.2$ Hz, ArH), 6.62 (2H, s, NH); ^{13}C NMR (DMSO-d_6) δ_H: 165.0 (1 × C), 163.9 (1 × C), 163.5 (1 × C), 148.0 (2 × C), 135.1 (1 × C), 131.9 (1 × C), 130.4 (1 × C), 128.7 (2 × C), 128.5 (1 × C), 126.9 (2 × C), 125.4 (1 × C), 100.0 (1 × C); Anal. calcd. for $C_{15}H_{12}N_4$: C, 72.56; H, 4.87; N, 22.57. Found: C, 72.50; H, 4.82; N, 22.59

*General procedure for the synthesis of compounds **6a–m***

4-Phenyl-6-(pyridin-3-yl)pyrimidin-2-amine **5** (1 equiv) was dissolved into water (25 mL) and sodium carbonate (1 N) was added to adjust the pH to 8–10. Then selected sulfonyl chlorides (1 equiv) were added and the mixtures were stirred at room temperature, while the reaction pH of the mixtures were maintained to 8–10 by occasional addition of aqueous sodium carbonate solution. Progress and completion of the reactions were monitored by TLC. After the reactions were completed, mixtures were poured into a beaker and the pH was adjusted to 2.0 by slow careful addition of 1 N HCl solution. Targeted compounds were precipitated and were filtered and washed

with 50 mL distilled water. The products were recrystallized from methanol to get essentially pure products **6a–m**.

Microwave synthetic strategy

Microwave-assisted reactions are now well recognized and have gained popularity especially in process chemistry and in cases where usual methods require forcing conditions or prolonged reaction times. Microwaves have also shown an advantage when products may decompose under prolonged reaction conditions. The possibilities offered by microwave-assisted reactions are particularly attractive for multi-step synthesis and drug discovery process, where purification are highly desirable. Synthetic strategy is almost same except using microwave (400 W) at 190°C for 20 min at atmospheric pressure. Yields are almost the same as in conventional method but the reaction time is reduced about five folds under microwave conditions.

*2-Bromo-N-(4-phenyl-6-(pyridin-3-yl)pyrimidin-2-yl)-benzenesulfonamide (**6a**)*

White solid; yield: 69%; m.p. 141–143°C; IR (ν_{max}, KBr pellets, cm^{-1}): 3190 (N–H), 1295 (S=O), 1194 (C–N); ^{1}H NMR (DMSO-d_6) δ_H: 9.50 (1H, s), 7.85 (1H, d, $J = 11.2$ Hz), 7.81 (1H, s), 7.18 (1H, d, $J = 6.0$ Hz), 7.14 (1H, d, $J = 8.0$ Hz), 7.08 (3H, d, $J = 8.0$ Hz), 6.86 (4H, t, $J = 11.2$ Hz), 6.81 (1H, t, $J = 8.8$ Hz), 6.72 (1H, d, $J = 7.2$ Hz), 4.13 (1H, s); ^{13}C NMR (DMSO-d_6) δ_H: 169.4 (1 × C), 163.1 (2 × C), 148.9 (2 × C), 142.4 (1 × C), 136.6 (1 × C), 135.9 (1 × C), 134.3 (1 × C), 133.1 (1 × C), 131.5 (1 × C), 129.4 (4 × C), 127.7 (3 × C), 124.3 (1 × C), 120.9 (1 × C), 100.2 (1 × C); Anal. calcd. for $C_{21}H_{15}BrN_4O_2S$: C, 53.97; H, 3.24; N, 11.99; S, 6.86. Found: C, 53.95; H, 3.20; N, 11.87; S, 6.82.

*3-Bromo-N-(4-phenyl-6-(pyridin-3-yl)pyrimidin-2-yl)-benzenesulfonamide (**6b**)*

White solid; yield: 71%; m.p. 179–181°C; IR (ν_{max}, KBr pellets, cm^{-1}): 3245 (N–H), 1225 (S=O), 1124 (C–N); ^{1}H NMR (DMSO-d_6) δ_H: 9.20 (1H, s, ArH), 7.54 (1H, d, $J = 12.0$ Hz, ArH), 7.51 (1H, s, ArH), 6.88 (1H, d, $J = 6.0$ Hz, ArH), 6.84 (1H, d, $J = 8.0$ Hz, ArH), 6.78 (3H, d, $J = 8.0$ Hz, ArH), 6.57 (1H, d, $J = 12.8$ Hz, ArH), 6.53 (1H, d, $J = 5.2$ Hz, ArH), 6.51–6.41 (4H, m), 3.81 (1H, s, NH); ^{13}C NMR (DMSO-d_6) δ_H: 165.6 (1 × C), 163.5 (1 × C), 163.1 (1 × C), 148.1 (2 × C), 138.8 (1 × C), 137.5 (1 × C), 135.5 (1 × C), 135.1 (1 × C), 133.9 (1 × C), 131.4 (1 × C), 130.5 (4 × C), 128.8 (1 × C), 127.4 (2 × C), 126.4 (1 × C), 125.4 (1 × C), 100.0 (1 × C); Anal. calcd. for $C_{21}H_{15}BrN_4O_2S$: C, 53.97; H, 3.24; N, 11.99; S, 6.86. Found C, 53.92; H, 3.27; N, 11.89; S, 6.66.

*4-Bromo-N-(4-phenyl-6-(pyridin-3-yl)pyrimidin-2-yl)-benzenesulfonamide (**6c**)*

Light yellow solid; yield: 82%; m.p. 219–221°C; IR (ν_{max}, KBr pellets, cm^{-1}): 3355 (N–H), 1273 (S=O), 1074 (C–N); ^{1}H NMR (DMSO-d_6) δ_H: 9.00 (1H, s, ArH), 7.34 (1H, d, $J = 11.2$ Hz, ArH), 7.31 (1H, s, ArH), 6.69 (1H, d, $J = 6.0$ Hz, ArH), 6.64 (2H, d, $J = 8.0$ Hz, ArH), 6.58 (2H, d, $J = 8.0$ Hz, ArH), 6.37 (2H, d, $J = 12.2$ Hz, ArH), 6.32 (3H, m, ArH), 6.23 (1H, t, $J = 8.0$ Hz, ArH), 3.61 (1H, s, NH); ^{13}C NMR (DMSO-d_6) δ_H: 169.7 (1 × C), 163.1 (2 × C), 148.9 (2 × C), 139.7.3 (1 × C), 136.6 (1 × C), 133.4 (2 × C), 131.4 (2 × C), 129.6 (5 × C), 127.5 (3 × C), 124.2 (1 × C), 100.4 (1 × C); Anal.calcd. for $C_{21}H_{15}BrN_4O_2S$: C, 53.97; H, 3.24; N, 11.99; S, 6.86. Found C, 53.95; H, 3.09; N, 11.89; S, 6.81.

*2-Chloro-N-(4-phenyl-6-(pyridin-3-yl)pyrimidin-2-yl)-benzenesulfonamide (**6d**)*

Light brown solid; yield: 73%; m.p. 150–152°C; IR (ν_{max}, KBr pellets, cm^{-1}): 3303 (N–H), 1354 (S=O), 1112 (C–N); ^{1}H NMR (DMSO-d_6) δ_H: 8.90 (1H, s, ArH), 7.68 (1H, d, $J = 9.0$ Hz, ArH), 7.61 (1H, d, $J = 6.0$ Hz, ArH), 7.51 (1H, s, ArH), 7.27 (4H, d, $J = 7.2$ Hz, ArH), 7.23 (4H, t, $J = 6.0$ Hz, ArH), 7.16 (2H, t, $J = 6.0$ Hz, ArH), 4.33 (1H, s, NH); ^{13}C NMR (DMSO-d_6) δ_H: 167.9 (1 × C), 162.9 (2 × C), 147.3 (2 × C), 139.1 (1 × C), 135.4 (1 × C), 134.3 (2 × C), 133.3 (2 × C), 131.1 (1 × C), 130.4 (1 × C), 129.6 (1 × C), 128.3 (2 × C), 127.5 (3 × C), 124.8 (1 × C), 100.0 (1 × C); Anal. calcd. for $C_{21}H_{15}ClN_4O_2S$: C, 59.64; H, 3.58; N, 13.25; S, 7.58. Found C, 59.62; H, 3.47; N, 13.31; S, 7.55.

*3-Chloro-N-(4-phenyl-6-(pyridin-3-yl)pyrimidin-2-yl)-benzenesulfonamide (**6e**)*

Brown solid; yield: 69%; m.p. 171–173°C; IR (ν_{max}, KBr pellets, cm^{-1}): 3278 (N–H), 1362 (S=O), 1089 (C–N); ^{1}H NMR (DMSO-d_6) δ_H: 8.21 (1H, s, ArH), 8.10 (1H, d, $J = 3.0$ Hz, ArH), 7.98 (1H, d, $J = 8.4$ Hz, ArH), 7.75 (1H, s, ArH), 7.70 (1H, s, ArH), 7.62 (1H, d, $J = 5.1$ Hz, ArH), 7.53 (3H, d, $J = 9.0$ Hz, ArH), 7.24 (1H, d, $J = 9.0$ Hz, ArH), 7.07 (3H, t, $J = 12.0$ Hz, ArH), 6.81 (1H, d, $J = 6.0$ Hz, ArH), 4.00 (1H, s, NH); ^{13}C NMR (DMSO-d_6) δ_H: 167.8 (1 × C), 162.2 (2 × C), 147.1 (2 × C), 141.5 (1 × C), 135.8 (1 × C), 134.1 (2 × C), 133.9 (1 × C), 132.1 (1 × C), 130.9 (1 × C), 129.5 (2 × C), 128.3 (1 × C), 127.2 (2 × C), 126.5 (1 × C), 125.1 (1 × C), 124.7 (1 × C), 99.7 (1 × C); Anal. calcd. for $C_{21}H_{15}ClN_4O_2S$: C, 59.64; H, 3.58; N, 13.25; S, 7.58. Found C, 59.66; H, 3.57; N, 13.15; S, 7.53.

*4-Chloro-N-(4-phenyl-6-(pyridin-3-yl)pyrimidin-2-yl)-benzenesulfonamide (**6f**)*

Dark brown solid; yield: 77%; m.p. 194–196°C; IR (ν_{max}, KBr pellets, cm^{-1}): 3254 (N–H), 1343 (S=O), 1074 (C–N); ^{1}H NMR (DMSO-d_6) δ_H: 9.00 (1H, s, ArH), 8.01 (1H, d, $J = 6.0$ Hz, ArH), 8.87 (1H, d, $J = 3.0$ Hz, ArH), 7.72 (1H, s, ArH), 7.57 (4H, d, $J = 10.2$ Hz, ArH), 7.49 (2H, d, $J = 6.0$ Hz, ArH), 7.06–6.96 (3H, m, ArH), 7.45 (1H, t, $J = 12.0$ Hz, ArH), 4.13 (1H, s, NH); ^{13}C NMR (DMSO-d_6) δ_H: 168.3 (1 × C), 162.3 (2 × C), 147.7 (2 × C), 137.1 (2 × C), 135.4 (1 × C), 134.6 (1 × C), 133.6 (1 × C), 129.4 (4 × C), 128.9 (3 × C), 127.3 (2 × C), 124.7 (1 × C), 99.5 (1 × C); Anal. calcd. for $C_{21}H_{15}ClN_4O_2S$: C, 59.64; H, 3.58; N, 13.25; S, 7.58 Found C, 59.60; H, 3.51; N, 13.29; S, 7.55.

*2-Methyl-N-(4-phenyl-6-(pyridin-3-yl)pyrimidin-2-yl)-benzenesulfonamide (**6g**)*

White solid; yield: 61%; m.p. 200–202°C; IR (ν_{max}, KBr pellets, cm^{-1}): 3229 (N–H), 1363 (S=O), 1054 (C–N); ^{1}H NMR (DMSO-d_6) δ_H: 9.88 (1H, s, ArH), 9.86 (1H, d, $J = 7.6$ Hz, ArH), 9.70 (1H, s, ArH), 9.57 (1H, d, $J = 8.4$ Hz, ArH), 9.41 (4H, d, $J = 9.2$ Hz, ArH), 9.20 (3H, t, $J = 7.6$ Hz, ArH), 8.99 (2H, d, $J = 8.8$ Hz, ArH), 8.75

(1H, t, $J = 8.0$ Hz, ArH), 7.39 (2H, d, $J = 8.0$ Hz, ArH), 6.56 (1H, s, NH), 3.02 (3H, s, CH_3); ^{13}C NMR (DMSO-d_6) δ_H: 168.5 (1 × C), 161.4 (2 × C), 147.4 (2 × C), 138.5 (1 × C), 136.1 (1 × C), 135.7 (1 × C), 134.2 (1 × C), 133.8 (1 × C), 131.3 (2 × C), 129.7 (3 × C), 128.2 (1 × C), 127.4 (2 × C), 124.8 (1 × C), 120.5 (1 × C), 99.9 (1 × C), 22.7 (1 × C); Anal. calcd. for $C_{22}H_{18}N_4O_2S$: C, 65.65; H, 4.51; N, 13.92; S, 7.97. Found C, 65.63; H, 4.49; N, 13.83; S, 7.96.

*3-Methyl-N-(4-phenyl-6-(pyridin-3-yl)pyrimidin-2-yl)-benzenesulfonamide (**6h**)*
White solid; yield: 78%; m.p. 217–219°C; IR (ν_{max}, KBr pellets, cm^{-1}): 3286 (N–H), 1360 (S=O), 1061 (C–N); ^{1}H NMR (DMSO-d_6) δ_H: 9.55 (1H, s, ArH), 9.42 (1H, d, $J = 8.0$ Hz, ArH), 9.35 (1H, d, $J = 8.0$ Hz, ArH), 9.02 (1H, s, ArH), 8.93 (2H, d, $J = 6.8$ Hz, ArH), 8.89 (1H, d, $J = 8.4$ Hz, ArH), 8.81 (1H, d, $J = 8.0$ Hz, ArH), 8.72 (1H, d, $J = 8.0$ Hz, ArH), 8.07–7.94 (5H, m), 4.53 (1H, s, NH), 2.84 (3H, s, CH_3); ^{13}C NMR (DMSO-d_6) δ_H: 169.1 (1 × C), 162.5 (2 × C), 146.2 (2 × C), 139.6 (1 × C), 138.8 (1 × C), 135.8 (1 × C), 134.2 (1 × C), 133.0 (1 × C), 131.4 (1 × C), 129.3 (2 × C), 128.6 (2 × C), 127.4 (2 × C), 126.7 (1 × C), 124.1 (2 × C), 99.7 (1 × C), 21.1 (1 × C); Anal. calcd. for $C_{22}H_{18}N_4O_2S$: C, 65.65; H, 4.51; N, 13.92; S, 7.97. Found C, 65.66; H, 4.54; N, 13.89; S, 7.99.

*4-Methyl-N-(4-phenyl-6-(pyridin-3-yl)pyrimidin-2-yl)-benzenesulfonamide (**6i**)*
Light yellow solid; yield: 86%; m.p. 262–264°C; IR (ν_{max}, KBr pellets, cm^{-1}): 3313 (N–H), 1353 (S=O), 1101 (C–N); ^{1}H NMR (DMSO-d_6) δ_H: 9.48 (1H, s, ArH), 9.46 (1H, d, $J = 7.6$ Hz, ArH), 9.30 (1H, s, ArH), 9.17 (1H, d, $J = 8.4$ Hz, ArH), 9.01 (4H, d, $J = 9.2$ Hz, ArH), 8.80 (3H, t, $J = 7.6$ Hz, ArH), 8.59 (2H, d, $J = 8.8$ Hz, ArH), 8.35 (1H, t, $J = 8.0$ Hz, ArH), 6.99 (2H, d, $J = 8.0$ Hz, ArH), 6.16 (1H, s, NH), 2.62 (3H, s, CH_3); ^{13}C NMR (DMSO-d_6) δ_H: 168.6 (1 × C), 160.9 (2 × C), 146.2 (2 × C), 137.6 (1 × C), 136.8 (1 × C), 135.3 (1 × C), 134.0 (1 × C), 133.3 (1 × C), 129.8 (4 × C), 128.2 (3 × C), 127.5 (2 × C), 124.2 (1 × C), 99.7 (1 × C), 21.8 (1 × C); Anal. calcd. for $C_{22}H_{18}N_4O_2S$: C, 65.65; H, 4.51; N, 13.92; S, 7.97. Found C, 65.61; H, 4.47; N, 13.81; S, 7.96.

*N-(4-Phenyl-6-(pyridin-3-yl)pyrimidin-2-yl)-methanesulfonamide (**6j**)*
Grey solid; yield: 79%; m.p. 167–169°C; IR (ν_{max}, KBr pellets, cm^{-1}): 3329 (N–H), 1365 (S=O), 1092 (C–N); ^{1}H NMR (DMSO-d_6) δ_H: 9.28 (1H, s, ArH), 9.26 (1H, d, $J = 7.6$ Hz, ArH), 9.07 (1H, s, ArH), 8.95 (1H, d, $J = 8.4$ Hz, ArH), 8.82 (2H, d, $J = 9.2$ Hz, ArH), 8.55 (1H, t, $J = 3.6$ Hz, ArH), 8.37 (2H, d, $J = 4.8$ Hz, ArH), 8.13 (1H, t, $J = 11.2$ Hz, ArH), 6.82 (1H, s, NH), 2.17 (3H, s, CH_3); ^{13}C NMR (DMSO-d_6) δ_H: 168.5 (1 × C), 162.7 (2 × C), 147.3 (2 × C), 135.8 (1 × C), 134.2 (1 × C), 133.1 (1 × C), 129.1 (2 × C), 128.7 (1 × C), 127.5 (2 × C), 124.1 (1 × C), 99.7 (1 × C), 43.9 (1 × C); Anal. calcd. for $C_{16}H_{14}N_4O_2S$: C, 58.88; H, 4.32; N, 17.17; S, 9.82. Found C, 58.86; H, 4.18; N, 17.23; S, 9.75.

*N-(4-Phenyl-6-(pyridin-3-yl)pyrimidin-2-yl)ethanesulfonamide (**6k**)*
White solid; yield: 80%; m.p. 170–172°C; IR (ν_{max}, KBr pellets, cm^{-1}): 3387 (N–H), 1321 (S=O), 1079 (C–N); ^{1}H NMR (DMSO-d_6) δ_H: 9.08 (1H, s, ArH), 9.06 (1H, d, $J = 7.6$ Hz, ArH), 8.87 (1H, s, ArH), 8.71 (1H, d, $J = 12.4$ Hz, ArH), 8.53 (2H, d, $J = 5.2$ Hz, ArH), 8.33 (1H, t, $J = 8.0$ Hz, ArH), 8.15 (2H, d, $J = 4.4$ Hz, ArH), 7.91 (1H, t, $J = 4.4$ Hz, ArH), 6.78 (1H, s, NH), 3.01 (2H, q, CH_2), 2.21 (3H, t, $J = 6.2$ Hz, CH_3); ^{13}C NMR (DMSO-d_6) δ_H: 168.2 (1 × C), 162.5 (2 × C), 147.1 (2 × C), 135.8 (1 × C), 134.1 (1 × C), 133.1 (1 × C), 129.0 (2 × C), 128.7 (1 × C), 127.4 (2 × C), 124.1 (1 × C), 99.1 (1 × C), 52.6 (1 × C), 14.9 (1 × C); Anal. calcd. for $C_{17}H_{16}N_4O_2S$: C, 59.98; H, 4.74; N, 16.46; S, 9.42. Found C, 59.92; H, 4.71; N, 16.40; S, 9.47.

*4-tert-Butyl-N-(4-phenyl-6-(pyridin-3-yl)pyrimidin-2-yl)-benzenesulfonamide (**6l**)*
Pale yellow solid; yield: 54%; m.p. 320–322°C; IR (ν_{max}, KBr pellets, cm^{-1}): 3334 (N–H), 1311 (S=O), 1159 (C–N); ^{1}H NMR (DMSO-d_6) δ_H: 9.57 (1H, s, ArH), 8.47 (1H, d, $J = 7.2$ Hz, ArH), 8.41 (1H, d, $J = 9.0$ Hz, ArH), 8.22 (1H, s, ArH), 8.07 (4H, d, $J = 10.2$ Hz, ArH), 7.96–7.78 (3H, m, ArH), 7.69 (2H, d, $J = 6.6$ Hz, ArH), 7.44 (1H, t, $J = 7.2$ Hz, ArH), 4.03 (1H, s, NH), 2.07 (9H, s, CH_3); ^{13}C NMR (DMSO-d_6) δ_H: 168.8 (1 × C), 162.3 (2 × C), 154.5 (1 × C), 147.2 (2 × C), 136.8 (1 × C), 135.8 (1 × C), 134.0 (1 × C), 133.9 (1 × C), 129.2 (2 × C), 128.3 (3 × C), 127.1 (1 × C), 124.1 (2 × C), 123.6 (1 × C), 101.1 (1 × C), 34.2 (1 × C), 31.1 (3 × C); Anal. calcd. for $C_{25}H_{24}N_4O_2S$: C, 67.54; H, 5.44; N, 12.60; S, 7.21. Found C, 67.57; H, 5.33; N, 12.68; S, 7.34.

*N-(4-Phenyl-6-(pyridin-3-yl)pyrimidin-2-yl)-benzenesulfonamide (**6m**)*
Yellow solid; yield: 59%; m.p. 268–270°C; IR (ν_{max}, KBr pellets, cm^{-1}): 3350 (N–H), 1330 (S=O), 1094 (C–N); ^{1}H NMR (DMSO-d_6) δ_H: 9.05 (1H, s, ArH), 8.87 (1H, d, $J = 7.2$ Hz, ArH), 8.77 (1H, d, $J = 12.0$ Hz, ArH), 8.48 (1H, s, ArH), 8.43 (2H, d, $J = 6.0$ Hz, ArH), 8.37 (1H, t, $J = 12.0$ Hz, ArH), 8.24 (1H, t, $J = 6.0$ Hz, ArH), 7.50–7.48 (2H, m, ArH), 7.23–7.16 (3H, m, ArH), 3.93 (1H, s, NH); ^{13}C NMR (DMSO-d_6) δ_H: 169.8 (1 × C), 163.3 (2 × C), 148.2 (2 × C), 145.1 (1 × C), 136.8 (1 × C),134.0 (2 × C), 131.9.0 (1 × C), 129.2 (5 × C), 127.3 (4 × C), 124 (1 × C), 100.0 (1 × C); Anal. calcd. for $C_{21}H_{16}N_4O_2S$: C, 64.93; H, 4.15; N, 14.42; S, 8.25. Found C, 64.90; H, 4.19; N, 14.46; S, 8.15.

Biological evaluation

AChE and BChE assays
The AChE and BChE inhibition activity was determined according to the Ellman's method [41] with slight modifications. Total volume of the reaction mixture was 100 μL. It contained 60 μL Na_2HPO_4 buffer with concentration of 50 mM pH 7.7. Ten microliters of test compound (0.5 mM well^{-1}) was added, followed by the addition of 10 μL enzyme (AChE, 0.005 unit well^{-1}). The contents were mixed, pre-incubated for 10 min at 37°C and pre-read at 405 nm. The reaction was initiated by the addition of 10 μL of 0.5 mM well^{-1} substrate (acetylthiocholine iodide for AChE), followed by the addition of 10 μL DTNB (0.5 mM well^{-1}). After 30 min of incubation at 37°C, absorbance was measured at 405 nm. Synergy HT (BioTek, USA) 96-well plate reader was used in all experiments. All experiments were carried out with their

respective controls in triplicate. Eserine (0.5 mM well^{-1}) was used as a positive control. The percent inhibition was calculated by the help of following equation.

$$\text{Inhibition}(\%) = \frac{\text{Control} - \text{Test} \times 100}{\text{Control}}$$

IC_{50} values (concentration at which there is 50% enzyme inhibition) of compounds were calculated from that data using EZ–Fit Enzyme kinetics software (Perrella Scientific Inc. Amherst, USA).

Molecular modeling

Quantitative structure-activity relationship (QSAR)

The studied compounds were drawn using ChemDraw Ultra 8.0 software [42] and for each compound, the lowest energy conformation was obtained by means of MOPAC2012 program [43] embedded within VEGA-ZZ [44, 45]. The accurate energy minimization was achieved by Austin Model-1 (AM1) semiempirical force-field within MOPAC. The AM1 force-field is characterized by its high accuracy and coverage for wide range of atoms. Molecular descriptors calculations were carried-out using PaDEL-Descriptor software [46]. The software calculates large set of 1D-3D molecular descriptors (ca. 1875) of different classes including constitutional, topological, information indices, eigenvalue-based indices, radial distribution function (RDF), 2D/3D autocorrelation etc. The calculated descriptors were served as independent variables during QSAR model development. The logarithmic values of experimentally observed percent inhibition of AChE and BChE enzymes at 0.5 mM level were served as the dependent variable. The QSAR models were developed and validated employing the QSARINS software [47, 48]. Model development process was initiated by reducing co-linear variables (corr. $>$ 0.98) and excluding the descriptor showing higher pair-wise correlation with others. All subsets procedure was adapted for the first two variables. Next, the optimal combinations of variables ($>$2) relevant to the dependent variable under study were selected by means of genetic algorithm (GA). During the GA variables selection phase, the population size, maximum number of generations and mutation rate were set to 800, 2000, and 0.2, respectively. Multiple linear regression (GA-MLR) method was used for the final model building. The final models robustness were validated employing internal predictive measures based on Q^2_{LOO} (leave one-out), Q^2_{LMO} (leave many-out) and $R^2_{Y\text{-scr}}$ (*Y*-scrambling).

Docking and molecular dynamic simulation

Prior to molecular dynamic simulation, docking experiments were performed using the program AutoDock Vina [49]. The structures of AChE from *Torpedo californica* (PDB-ID: 3I6Z, 2.19 Å) and BChE from *Homo sapiens* (PDB-ID: 1P0I, 2.0 Å) were downloaded from Protein Data Bank [50]. The complexed inhibitors as well as water molecules were extracted from the initial X-ray structures. Later, AutoDock Tools (MGL Tools 1.5.6rc2) were used for adding polar hydrogens and generating Gasteiger charges. The accurately minimized compound (**4j**) was treated employing the previous mentioned procedure. Grid boxes were established to cover the active site of the macromolecules, with a spacing of 1.0 Å between the grid points, centered toward the coordinates of 1.08 (*x*), 63.49 (*y*), 67.43 (*z*) for AChE and 132.65 (*x*), 115.85 (*y*), 39.86 (*z*) for BChE. The exhaustiveness and the number of poses were set to 12 and 10, respectively.

Molecular dynamic simulations for the most potent compound **(6j)** with respect to AChE and BChE macromolecules were started from the earlier docked complexes. All-atoms molecular dynamic simulations were carried-out employing Desmond software v3.8 [51, 52] embedded within Maestro interface v9.8. OPLS_2005 force field parameters were used during all calculations. Each complex was subjected to the same dynamic protocol; in brief, the protein-ligand complex was solvated using TIP3P explicit water molecules as solvent model within an orthorhombic periodic boundary box of the size 10 Å^3; then, the system was neutralized by adding appropriate counter-ions followed by adding 0.15 M of salt to resemble the physiological conditions. Before applying the actual dynamic production run, the system was relaxed by performing a series of short (2000 iterations) restrained and non-restrained solute minimizations steps followed by short 12 ps simulation steps using NVT and NPT ensembles. Subsequently, the production run was carried-out for 20 ns using the NPT ensemble class integrating the equation of motion every 2 fs and setting the temperature and pressure to 300 K and 1 atmosphere, respectively. The short range interactions (van der Waals) cut-off was set to 9 Å, while the long range electrostatic interactions were calculated employing the particle mesh Ewald (PME) method. Trajectories were visualized within Maestro environment and the results were analyzed using Desmond interaction diagram panel.

We acknowledge Higher Education Commission of Pakistan for financial support under National Research Program for Universities (Project No.3971). We also acknowledge GC University Lahore, Pakistan to provide funds under Faculty Research Programme (Project No. 90/ORIC/15). Our gratitude extends to the E.D. Shaw Research Lab, Schrödinger®, Inc. and Professor Paola Gramatica for providing the licensed softwares.

The authors have declared no conflict of interest.

References

[1] S. Oddo, A. Caccamo, M. Kitazawa, B. P. Tseng, F. M. LaFerla, *Neurobiol. Aging*. **2003**, *24*, 1063–1070.
[2] A. P. Murray, M. B. Faraoni, M. J. Castro, N. P. Alza, V. Cavallaro, *Curr. Neuropharmacol*. **2013**, *11*, 388–413.
[3] A. Wimo, L. Jönsson, J. Bond, M. Prince, B. Winblad, A. D. International, *Alzheimers Dement*. **2013**, *9*, 1–11.

[4] S. W. Scheff, D. A. Price, *Neurobiol. Aging* **2003**, *24*, 1029–1046.
[5] D. M. Walsh, D. J. Selkoe, *Neuron* **2004**, *44*, 181–193.
[6] M. Weinstock, *Neurodegeneration* **1995**, *4*, 349–356.
[7] S. Akasofu, M. Kimura, T. Kosasa, K. Sawada, H. Ogura, *Chem. Biol. Interact*. **2008**, *175*, 222–226.
[8] F. Leonetti, M. Catto, O. Nicolotti, L. Pisani, A. Cappa, A. Stefanachi, A. Carotti, *Bioorg. Med. Chem*. **2008**, *16*, 7450–7456.
[9] R. Sheng, X. Lin, J. Li, Y. Jiang, Z. Shang, Y. Hu, *Bioorg. Med. Chem. Lett*. **2005**, *15*, 3834–3837.
[10] H. Sugimoto, *Chem. Rec*. **2001**, *1*, 63–73.
[11] M. W. Jann, *Pharmacotherapy* **2000**, *20*, 1–12.
[12] V. Zarotsky, J. J. Sramek, N. R. Cutler, *Am. J. Health Syst. Pharm*. **2003**, *60*, 446–452.
[13] P. N. Tariot, H. J. Federoff, *Alzheimer Dis. Assoc. Disord*. **2003**, *17*, S105–S113.
[14] C. P. Smith, G. M. Bores, W. Petko, M. Li, D. E. Selk, D. K. Rush, F. Camacho, J. T. Winslow, R. Fishkin, D. M. Cunningham, *J. Pharm. Exp. Ther*. **1997**, *280*, 710–720.
[15] R. S. Doody, *Alzheimer Dis. Assoc. Disord*. **1999**, *13*, S20–S26.
[16] P. Camps, X. Formosa, C. Galdeano, T. Gómez, D. Munoz-Torrero, M. Scarpellini, E. Viayna, A. Badia, M. V. Clos, A. Camins, *J. Med. Chem*. **2008**, *51*, 3588–3598.
[17] X. Chen, I. G. Tikhonova, M. Decker, *Bioorg. Med. Chem*. **2011**, *19*, 1222–1235.
[18] L. Huang, Z. Luo, F. He, J. Lu, X. Li, *Bioorg. Med. Chem*. **2010**, *18*, 4475–4484.
[19] P. Meena, V. Nemaysh, M. Khatri, A. Manral, P. M. Luthra, M. Tiwari, *Bioorg. Med. Chem*. **2015**, *23*, 1135–1148.
[20] F. Rahim, M. T. Javed, H. Ullah, A. Wadood, M. Taha, M. Ashraf, M. A. Khan, F. Khan, S. Mirza, K. M. Khan, *Bioorg. Chem*. **2015**, *62*, 106–116.
[21] P. R. Carlier, E.S.-H. Chow, Y. Han, J. Liu, J. E. Yazal, Y.-P. Pang, *J. Med. Chem*. **1999**, *42*, 4225–4231.
[22] E. Arias, S. Gallego-Sandín, M. Villarroya, A. G. García, M. G. López, *J. Pharmacol. Exp. Ther*. **2005**, *315*, 1346–1353.
[23] R. Annicchiarico, A. Federici, C. Pettenati, C. Caltagirone, *Ther. Clin. Risk Manag*. **2007**, *3*, 1113.
[24] C. G. Carolan, G. P. Dillon, J. M. Gaynor, S. Reidy, S. A. Ryder, D. Khan, J. F. Marquez, J. F. Gilmer, *J. Med. Chem*. **2008**, *51*, 6400–6409.
[25] Z. Radic, N. A. Pickering, D. C. Vellom, S. Camp, P. Taylor, *Biochemistry* **1993**, *32*, 12074–12084.
[26] D. Karlsson, A. Fallarero, G. Brunhofer, P. Guzik, M. Prinz, U. Holzgrabe, T. Erker, P. Vuorela, *Eur. J. Pharm. Sci*. **2012**, *45*, 169–183.
[27] J. Grutzendler, J. C. Morris, *Drugs* **2001**, *61*, 41–52.
[28] S. Hawser, S. Lociuro, K. Islam, *Biochem. Pharmacol*. **2006**, *71*, 941–948.
[29] R. J. Milling, C. J. Richardson, *Pestic. Sci*. **1995**, *45*, 43–48.
[30] J. Bernier, J. Henichart, V. Warin, F. Baert, *J. Pharm. Sci*. **1980**, *69*, 1343–1345.
[31] B. Gong, F. Hong, C. Kohm, S. Jenkins, J. Tulinsky, R. Bhatt, P. de Vries, J. W. Singer, P. Klein, *Bioorg. Med. Chem. Lett*. **2004**, *14*, 2303–2308.
[32] L. S. Jeong, L. X. Zhao, W. J. Choi, S. Pal, Y. H. Park, S. K. Lee, M. W. Chun, Y. B. Lee, C. H. Ahn, H. R. Moon, *Nucleosides Nucleotides Nucleic Acids* **2007**, *26*, 713–716.
[33] V. R. Gadhachanda, B. Wu, Z. Wang, K. L. Kuhen, J. Caldwell, H. Zondler, H. Walter, M. Havenhand, Y. He, *Bioorg. Med. Chem. Lett*. **2007**, *17*, 260–265.
[34] D. Hocková, A. Holý, M. Masojídková, G. Andrei, R. Snoeck, E. De Clercq, J. Balzarini, *J. Med. Chem*. **2003**, *46*, 5064–5073.
[35] H.-X. Dai, A. F. Stepan, M. S. Plummer, Y.-H. Zhang, J.-Q. Yu, *J. Am. Chem. Soc*. **2011**, *133*, 7222–7228.
[36] H. Göçer, A. Akıncıoğlu, N. Öztaşkın, S. Göksu, İ. Gülçin, *Arch. Pharm*. **2013**, *346*, 783–792.
[37] G. Renzi, A. Scozzafava, C. T. Supuran, *Bioorg. Med. Chem. Lett*. **2000**, *10*, 673–676.
[38] S. Riaz, I. U. Khan, M. Bajda, M. Ashraf, A. Shaukat, T. U. Rehman, S. Mutahir, S. Hussain, G. Mustafa, M. Yar, *Bioorg. Chem*. **2015**, *63*, 64–71.
[39] M. Yar, M. Bajda, R. A. Mehmood, L. R. Sidra, N. Ullah, L. Shahzadi, M. Ashraf, T. Ismail, S. A. Shahzad, Z. A. Khan, *Lett. Drug Des. Discov*. **2014**, *11*, 331.
[40] A. Nie, J. Wang, Z. Huang, *J. Comb. Chem*. **2006**, *8*, 646–648.
[41] G. L. Ellman, K. D. Courtney, V. Andres, R. M. Featherstone, *Biochem. Pharmacol*. **1961**, *7*, 88–95.
[42] http://www.cambridgesoft.com.
[43] J.J.P.S. MOPAC2012, Stewart Computational Chemistry, version 15.321, w. http://OpenMOPAC.net.
[44] A. Pedretti, L. Villa, G. Vistoli, *Theor. Chem. Acc*. **2003**, *109*, 229–232.
[45] A. Pedretti, L. Villa, G. Vistoli, *J. Comput. Aided Mol. Des*. **2004**, *18*, 167–173.
[46] C. W. Yap, *J. Comput. Chem*. **2011**, *32*, 1466–1474.
[47] P. Gramatica, S. Cassani, N. Chirico, *J. Comput. Chem*. **2014**, *35*, 1036–1044.
[48] P. Gramatica, N. Chirico, E. Papa, S. Cassani, S. Kovarich, *J. Comput. Chem*. **2013**, *34*, 2121–2132.
[49] O. Trott, A. J. Olson, *J. Comput. Chem*. **2010**, *31*, 455–461.
[50] http://www.rcsb.org/pdb/.
[51] K. J. Bowers, E. Chow, H. Xu, R. O. Dror, M. P. Eastwood, B. A. Gregersen, J. L. Klepeis, I. Kolossvary, M. A. Moraes, F. D. Sacerdoti, J. K. Salmon, Y. Shan, D. E. Shaw, Proceedings of the ACM/IEEE Conference on Supercomputing (SC06), Tampa, Florida, November, 11-17, **2006**.
[52] Desmond Molecular Dynamics System, version3.8, D. E. Shaw Research, New York, NY, **2014**.